

Efficient Alternating Least Squares Algorithms for Truncated HOSVD of Higher-Order Tensors

Chuanfu Xiao · Chao Yang · Min Li

Received: date / Accepted: date

Abstract The truncated Tucker decomposition, also known as the truncated higher-order singular value decomposition (HOSVD), has been extensively utilized as an efficient tool in many applications. Popular direct methods for truncated HOSVD often suffer from the notorious intermediate data explosion issue and are not easy to parallelize. In this paper, we propose a class of new truncated HOSVD algorithms based on alternating least squares (ALS). The proposed ALS-based approaches are able to eliminate the redundant computations of the singular vectors of intermediate matrices and are therefore free of data explosion. Also, the new methods are more flexible with adjustable convergence tolerance and are intrinsically parallelizable on high-performance computers. Theoretical analysis reveals that the ALS iteration in the proposed algorithms is q -linear convergent with a relatively wide convergence region. Numerical experiments with both synthetic and real-world tensor data demonstrate that ALS-based methods can substantially reduce the total cost of the original ones and are highly scalable for parallel computing.

Keywords Tucker decomposition · Truncated higher-order singular value decomposition · Best low multilinear rank approximation · Alternating least squares · Parallelization

Mathematics Subject Classification (2010) 15A69 · 49M27 · 65D15 · 65F55

1 Introduction

As a natural extension of vectors (order one) and matrices (order two), higher-order tensors have been receiving increasingly more attention in various applications, such as signal processing [16, 50],

Chuanfu Xiao
School of Mathematical Sciences, Peking University, Beijing 100871, China
E-mail: chuanfuxiao@pku.edu.cn

Chao Yang (✉)
School of Mathematical Sciences, Peking University, Beijing 100871, China
E-mail: chao.yang@pku.edu.cn

Min Li
Institute of Software, Chinese Academy of Sciences, Beijing 100190, China
E-mail: limin2016@iscas.ac.cn

computer vision [49, 57, 58], chemometrics [25, 31, 9], deep learning [12, 40], and scientific computing [8, 32, 23]. For decades, tensor decompositions have been extensively utilized as an efficient tool for dimension reductions, latent variable analysis and other purposes in a wide range of scientific and engineering fields [23, 7, 35, 29, 27, 19]. There exist a number of tensor decomposition models, such as canonical polyadic (CP) decomposition [26, 11, 33], also known as CANDECOMP/PARAFAC decomposition, Tucker decomposition [55, 37, 14], tensor train (TT) model [43], and hierarchical Tucker (HT) model [22, 24, 42]. Among them, the Tucker decomposition, also known as the higher-order singular value decomposition (HOSVD), is regarded as a generalization of the matrix SVD and has been applied with significant successes in many applications [55, 37, 14, 16, 29, 34].

In both theory and practice, a commonly considered problem is the truncated Tucker decomposition, which satisfies

$$\min_{\mathcal{B}} \|\mathcal{A} - \mathcal{B}\|, \quad (1.1)$$

where $\mathcal{A} \in \mathbb{R}^{I_1 \times I_2 \times \dots \times I_N}$ is a given order N tensor and $\mathcal{B} \in \mathbb{R}^{I_1 \times I_2 \times \dots \times I_N}$ is its low multilinear rank approximation [14, 34]. Existing approaches solving (1.1) can be roughly divided into two categories: *direct* and *iterative* methods. The most popular direct algorithms for the low multilinear rank approximation of higher-order tensors is the truncated HOSVD (t -HOSVD) [55, 15] and its improved version, the sequentially truncated HOSVD (st -HOSVD) [56]. Despite the fact that the results of t -HOSVD and st -HOSVD are usually suboptimal, they can serve as good initial solution for popular iterative methods such as higher-order orthogonal iteration (HOOI) [36, 15]. Other than the HOOI method, some efforts are also made in developing second-order approaches, such as Newton-type [20, 47, 30] and trust-region [29, 28] algorithms. Although these methods can achieve faster convergence under certain conditions, they are still in early study and are usually not suitable for large-scale tensors [62].

In this paper, we focus on study how to efficiently compute the truncated Tucker decomposition (1.1) of higher-order tensors by using the direct algorithms, i.e., t -HOSVD and st -HOSVD. As a major cost of the two algorithms, the computation of tensor-matrix multiplications has been extensively optimized in a number of high-performance tensor libraries [44, 38, 51, 48]. Another potential bottleneck of the t -HOSVD and st -HOSVD algorithms is the calculation of the singular vectors of the intermediate matrices, which can be done by the truncated matrix SVD or eigen-decomposition of Gram matrix [36, 15, 34, 4, 41]. The truncated matrix SVD can be obtained by using Krylov subspace methods [21, 13, 6], whilst the eigen-decomposition of the symmetric nonnegative definite Gram matrix can be done with a Krylov-Schur algorithm [52, 53, 61, 21]. Due to the fact that these methods rely on the factorization of intermediate matrices, they suffer from the notorious *data explosion* issue [4, 41]. And even if the hardware storage allowed, they are still not scalable for parallel computing and the total computation cost could be unbearably high.

In order to improve the performance of the t -HOSVD and st -HOSVD algorithms, we propose a class of alternating least squares (ALS) based algorithms for solving the truncated HOSVD problem. The key observation is that in the original algorithms the computations of singular vectors of the intermediate matrices are indeed not necessary and can be replaced with low rank approximations, and the low rank approximations can be done by using an ALS method which does not explicitly require the intermediate matrices. The proposed ALS-based algorithms enjoy advantages such as low computational cost, adjustable tolerance control, easy parallelization, and total avoidance of the intermediate data explosion issue. We present theoretical analysis and show that the ALS iteration in the proposed algorithms is q -linear convergent with a relatively wide convergence region.

Several numerical experiments with both synthetic and real-world tensor data demonstrate that new algorithms can substantially reduce the total cost of the original ones and are highly parallelizable.

The organization of the paper is as follows. In Sec. 2, we introduce some basic notations of tensor and the corresponding algorithms. In Sec. 3, the t -HOSVD-ALS and st -HOSVD-ALS algorithms are proposed. Some theoretical analysis on the convergence behavior of the ALS methods can also be found in Sec. 3. After that, computational complexity and the approximation errors of proposed algorithms are analyzed in Sec. 4. Test results on several numerical experiments are reported in Sec. 5. And the paper is concluded in Sec. 6.

2 Notations and Nomenclatures

Symbols frequently used in this paper can be found in the following table.

Symbols	Notations
a	scalar
\mathbf{a}	vector
\mathbf{A}	matrix
\mathcal{A}	three or higher-order tensor
\circ	vector outer product
\times_n	mode- n product of tensor and matrix
\mathbf{I}_n	identity matrix with size $n \times n$
$I_{n:N}$	$\prod_{i=n}^N I_i$
$\mathcal{R}(\mathbf{A})$	a subspace formed by the columns of matrix \mathbf{A}
$\sigma(\mathbf{A})$	a set that consists of singular values of matrix \mathbf{A}
\mathbf{A}^\dagger	pseudo-inverse of matrix \mathbf{A}

Given an order N tensor $\mathcal{A} \in \mathbb{R}^{I_1 \times I_2 \times \cdots \times I_N}$, we denote $\mathcal{A}_{i_1, i_2, \dots, i_N}$ as its (i_1, i_2, \dots, i_N) -th element. In particular, rank one tensor is denoted as

$$\mathbf{u}_1 \circ \mathbf{u}_2 \circ \cdots \circ \mathbf{u}_N,$$

where $\mathbf{u}_n \in \mathbb{R}^{I_n}$ is a vector.

The norm of tensor \mathcal{A} is defined as

$$\|\mathcal{A}\|_F = \sqrt{\sum_{i_1, i_2, \dots, i_N} \mathcal{A}_{i_1, i_2, \dots, i_N}^2}.$$

The matricization of a higher-order tensor is a process of reordering the elements of the tensor into a matrix. For example, the mode- n matricization of tensor \mathcal{A} is denoted as $\mathbf{A}_{(n)}$, which is a matrix belonging to $\mathbb{R}^{I_n \times (I_1 \cdots I_{n-1} I_{n+1} \cdots I_N)}$. Specifically, the (i_1, i_2, \dots, i_N) -th element of tensor \mathcal{A} is mapped to the (i_n, j) -th entry of matrix $\mathbf{A}_{(n)}$, where

$$j = 1 + \sum_{k=1, k \neq n}^N (i_k - 1) J_k \quad \text{with} \quad J_k = \prod_{m=1, m \neq n}^{k-1} I_m.$$

The multilinear rank of a higher-order tensor \mathcal{A} is an integer array (R_1, R_2, \dots, R_N) , where R_n is the rank of its mode- n matricization $\mathbf{A}_{(n)}$.

A frequently encountered operation in tensor computation is the tensor-matrix multiplication. In particular, the mode- n tensor-matrix multiplication refers to the contraction of the tensor with a matrix along the n -th index. For example, suppose that $\mathbf{U} \in \mathbb{R}^{J \times I_n}$ is a matrix, the mode- n product of \mathcal{A} and \mathbf{U} is denoted as $\mathcal{A} \times_n \mathbf{U} \in \mathbb{R}^{I_1 \times \dots \times I_{n-1} \times J \times I_{n+1} \times \dots \times I_N}$. Elementwisely, one has

$$\mathcal{B}_{i_1, \dots, j, \dots, i_N} = (\mathcal{A} \times_n \mathbf{U})_{i_1, \dots, j, \dots, i_N} = \sum_{i_n=1}^{I_n} \mathcal{A}_{i_1, \dots, i_n, \dots, i_N} \mathbf{U}_{j, i_n}.$$

The Tucker decomposition [55, 37], also known as the higher-order singular value decomposition (HOSVD) [14], is formally defined as

$$\mathcal{A} = \mathcal{G} \times_1 \mathbf{U}^{(1)} \times_2 \mathbf{U}^{(2)} \dots \times_N \mathbf{U}^{(N)},$$

where $\mathcal{G} \in \mathbb{R}^{R_1 \times R_2 \times \dots \times R_N}$ is referred to as the core tensor and $\mathbf{U}^{(n)} \in \mathbb{R}^{I_n \times R_n}$ are column orthogonal with each other for all $n \in \{1, 2, \dots, N\}$. We remark here that the size of the core tensor is often smaller than that of the original tensor, though it is hard to know how small it can be a priori [18, 34]. In many applications, the Tucker decomposition is usually applied in its truncated form, which reads

$$\begin{aligned} \min_{\mathcal{G}; \mathbf{U}^{(1)}, \mathbf{U}^{(2)}, \dots, \mathbf{U}^{(N)}} \|\mathcal{A} - \mathcal{G} \times_1 \mathbf{U}^{(1)} \times_2 \mathbf{U}^{(2)} \dots \times_N \mathbf{U}^{(N)}\|, \\ \text{s.t. } \mathbf{U}^{(n)T} \mathbf{U}^{(n)} = \mathbf{I}_{R_n}, \quad n \in \{1, 2, \dots, N\} \end{aligned} \quad (2.1)$$

where (R_1, R_2, \dots, R_N) is a pre-determined truncation, smaller than the size of original tensor. Suppose that the exact solution of (2.1) is $\mathbf{U}^{*(1)}, \mathbf{U}^{*(2)}, \dots, \mathbf{U}^{*(N)}$, and \mathcal{G}^* , then it is easy to see that

$$\mathcal{G}^* = \mathcal{A} \times_1 (\mathbf{U}^{*(1)})^T \times_2 (\mathbf{U}^{*(2)})^T \dots \times_N (\mathbf{U}^{*(N)})^T,$$

which means

$$\mathcal{A} \times_1 (\mathbf{U}^{*(1)}) (\mathbf{U}^{*(1)})^T \times_2 (\mathbf{U}^{*(2)}) (\mathbf{U}^{*(2)})^T \dots \times_N (\mathbf{U}^{*(N)}) (\mathbf{U}^{*(N)})^T \quad (2.2)$$

is the best low multilinear rank approximation of \mathcal{A} .

To compute the best low multilinear rank approximation of a higher-order tensor in the truncated Tucker decomposition, a popular approach is the truncated HOSVD (t -HOSVD, [55]) originally presented by Tucker himself [55]. Nowadays, it is better known with the effort of Lathauwer *et al.* [15], who analyzed the structure of core tensor and proposed to employ truncated SVD of the intermediate matrices in truncated HOSVD. The computing procedure of t -HOSVD is given in Algorithm 1.

Algorithm 1 t -HOSVD [55, 15]

Input: Tensor $\mathcal{A} \in \mathbb{R}^{I_1 \times I_2 \times \dots \times I_N}$, truncation (R_1, R_2, \dots, R_N)

Output: Low multilinear rank approximation $\hat{\mathcal{A}} \approx \mathcal{G} \times_1 \mathbf{U}^{(1)} \times_2 \mathbf{U}^{(2)} \dots \times_N \mathbf{U}^{(N)}$

- 1: **for all** $n \in \{1, 2, \dots, N\}$ **do**
 - 2: Compute $\mathbf{Q} \in \mathbb{R}^{I_n \times R_n}$ which is comprised of the R_n leading left singular vectors of $\mathbf{A}_{(n)}$
 - 3: $\mathbf{U}^{(n)} = \mathbf{Q}$
 - 4: **end for**
 - 5: $\mathcal{G} = \mathcal{A} \times_1 \mathbf{U}^{(1)T} \times_2 \mathbf{U}^{(2)T} \dots \times_N \mathbf{U}^{(N)T}$
-

We remark here that \mathbf{Q} can also be obtained by computing the R_n eigenvectors of the Gram matrix $\mathbf{A}_{(n)}\mathbf{A}_{(n)}^T$. It is clear that t -HOSVD can be seen as a natural extension of the truncated SVD of a matrix to higher-order tensors. But unlike the matrix case, the approximation error of t -HOSVD is quasi-optimal [55, 15, 34, 56].

As a subsequent improvement of t -HOSVD, the sequentially truncated HOSVD (st -HOSVD), proposed by Vannieuwenhoven *et al.* [56] uses a different truncation strategy, as shown in Algorithm 2.

Algorithm 2 st -HOSVD [56]

Input: Tensor $\mathbf{A} \in \mathbb{R}^{I_1 \times I_2 \times \dots \times I_N}$, truncation (R_1, R_2, \dots, R_N)

Output: Low multilinear rank approximation $\hat{\mathbf{A}} \approx \mathbf{G} \times_1 \mathbf{U}^{(1)} \times_2 \mathbf{U}^{(2)} \dots \times_N \mathbf{U}^{(N)}$

1: Select an order of $\{1, 2, \dots, N\}$, i.e., $\{i_1, i_2, \dots, i_N\}$.

Let $\mathbf{B} = \mathbf{A}$

2: **for all** $n \in \{i_1, i_2, \dots, i_N\}$ **do**

3: Compute $\mathbf{Q} \in \mathbb{R}^{I_n \times R_n}$ which is comprised of the R_n leading left singular vectors of $\mathbf{B}_{(n)}$

4: $\mathbf{U}^{(n)} = \mathbf{Q}$

5: Update $\mathbf{B} = \mathbf{B} \times_n \mathbf{U}^{(n)T}$

6: **end for**

7: $\mathbf{G} = \mathbf{A} \times_1 \mathbf{U}^{(1)T} \times_2 \mathbf{U}^{(2)T} \dots \times_N \mathbf{U}^{(N)T}$

Analogous to t -HOSVD, in st -HOSVD one can also obtain \mathbf{Q} by computing the R_n eigenvectors of the Gram matrix $\mathbf{B}_{(n)}\mathbf{B}_{(n)}^T$. Comparing with t -HOSVD, st -HOSVD introduces more tensor-matrix multiplications, but greatly reduces the size of the intermediate matrices. The approximation error of st -HOSVD, though still quasi-optimal, can sometimes be smaller than that of t -HOSVD, according to the numerical results in [56].

It is worth mentioning that the order of $\{1, 2, \dots, N\}$ in Algorithm 2 could have a strong influence on the computational cost and approximation error of st -HOSVD. But there is no theoretical guidance on how to select the order. From the viewpoint of computational cost, we have a simple suggestion, summarized in the following proposition.

Proposition 1 *Let $\mathbf{A} \in \mathbb{R}^{I_1 \times I_2 \times \dots \times I_N}$ be an N -order tensor, and the multilinear rank is (R_1, R_2, \dots, R_N) . Without loss of generality, suppose that $I_n \approx I$ for any $n \in \{1, 2, \dots, N\}$, and $R_1 \leq R_2 \leq \dots \leq R_N$. Then the computational cost of the st -HOSVD algorithm based on order $\{1, 2, \dots, N\}$ is less than the that based on order $\{N, \dots, 2, 1\}$.*

Proof. If we select $\{1, 2, \dots, N\}$ as the order of Algorithm 2, when applying a Krylov subspace method to compute the truncated matrix SVD, the computational cost is

$$\mathcal{O}\left(\sum_{n=1}^N R_{1:n} I_{n:N}\right) \approx \mathcal{O}\left(\sum_{n=1}^N R_{1:n} I^{N-n+1}\right), \quad (2.3)$$

Similarly, the computational cost when we select $(N, \dots, 2, 1)$ as the order of Algorithm 2 is

$$\mathcal{O}\left(\sum_{n=1}^N R_{n:N} I_{1:n}\right) \approx \mathcal{O}\left(\sum_{n=1}^N R_{n:N} I^n\right). \quad (2.4)$$

Clearly, (2.4) is smaller than (2.3). \square

For the best low multilinear rank approximation (2.1), it is easy to see that $\mathbf{U}^{*(n)}$ is a column orthogonal factor matrix, therefore $(\mathbf{U}^{*(n)})(\mathbf{U}^{*(n)})^T$ represents the orthogonal projection of subspace $\mathcal{R}(\mathbf{U}^{*(n)})$. Consequently, subspace represented by the optimal factor matrices are critical. Truncated SVD and eigen-decomposition are the commonly applied approaches to determine this subspace in the original t -HOSVD and st -HOSVD procedures, both of which have advantages and disadvantages. For instance, the truncated SVD has less computational complexity and can avoid the intermediate data explosion when an implicit algorithm is used, but is hard to parallelize. Eigen-decomposition, on the other hand, is more parallelization friendly than truncated SVD, but suffers from the intermediate data explosion issue and induces more computational cost.

In addition to truncated SVD or eigen-decomposition, tensor matricization and tensor-matrix multiplication are also important in the original t -HOSVD and st -HOSVD algorithms. Recently, some efforts on high-performance optimizations of basic tensor operations are made. For example, Li *et al.* proposed a shared-memory parallel implementation of dense tensor-matrix multiplication [38], and Smith *et al.* considered sparse tensor-matrix multiplications [51]. Nevertheless, the calculation of truncated SVD or eigen-decomposition is still the major challenge in the t -HOSVD and st -HOSVD algorithms.

3 Alternating Least Squares Algorithms for t -HOSVD and st -THOSVD

In this paper we tackle the challenges of the original t -HOSVD and st -HOSVD algorithms from an alternating least squares (ALS) perspective. Instead of utilizing truncated SVD or eigen-decomposition on the intermediate matrices, we propose to compute the dominant subspace with an ALS algorithm to solve a closely related matrix low rank approximation problem. The new method is referred to as t -HOSVD-ALS and st -HOSVD-ALS, respectively. Compared with the original t -HOSVD and st -HOSVD, the proposed algorithms enjoy advantages such as low computational cost, easy to parallelize, and free of the intermediate data explosion issue.

The classical ALS method for solving matrix low rank approximation problems was originally proposed by Leeuw et al., [17] and further applied in principal component analysis [63]. Algorithm 3 shows the detailed procedure of the ALS method.

Algorithm 3 $[\mathbf{L}^*, \mathbf{R}^*] = \text{ALS}(\mathbf{A}, r)$

Input: Matrix $\mathbf{A} \in \mathbb{R}^{m \times n}$, truncation $r < \min\{m, n\}$

Initial guesses $\mathbf{L}_0 \in \mathbb{R}^{m \times r}$ or $\mathbf{R}_0 \in \mathbb{R}^{n \times r}$

Output: Low rank approximation $\hat{\mathbf{A}} = \mathbf{L}^* \mathbf{R}^{*T}$

- 1: $k = 0$
 - 2: **while** not convergent **do**
 - 3: Solving multi-side least squares problem $\min_{\mathbf{R}} \|\mathbf{L}_k \mathbf{R}^T - \mathbf{A}\|_F^2$
 - 4: $\mathbf{R}_k = (\mathbf{A}^T \mathbf{L}_k)(\mathbf{L}_k^T \mathbf{L}_k)^{-1}$
 - 5: Solving multi-side least squares problem $\min_{\mathbf{L}} \|\mathbf{R}_k \mathbf{L}^T - \mathbf{A}^T\|_F^2$
 - 6: $\mathbf{L}_{k+1} = (\mathbf{A} \mathbf{R}_k)(\mathbf{R}_k^T \mathbf{R}_k)^{-1}$
 - 7: $k = k + 1$
 - 8: **end while**
-

As an iterative method, the number of iterations for the ALS method has a dependency on the initial guess and the convergence criterion [54]. In what follows we will establish a rigorous convergence theory of the ALS method and derive an evaluation of the convergence region, which can help understand how the initial guess could affect the speed of convergence.

To establish the convergence theory of the ALS method, we first require the following lemma, which was proved in [60].

Lemma 1 *Let \mathbf{A} , $\mathbf{B} \in \mathbb{R}^{n \times n}$ be symmetric positive definite matrices and satisfy*

$$\mathbf{B} \leq \mathbf{A},$$

then the following inequalities hold

$$\|\mathbf{A}^{-1}\mathbf{B}\|_2 \leq 1 \text{ and } \|\mathbf{B}\mathbf{A}^{-1}\|_2 \leq 1,$$

where $\mathbf{B} \leq \mathbf{A}$ represents $\mathbf{A} - \mathbf{B}$ is symmetric semi-positive matrix.

The convergence theorem of Algorithm 3 is summarized in the theorem below.

Theorem 1 *Let $\mathbf{A} \in \mathbb{R}^{m \times n}$ be a matrix, and $\sigma_1 \geq \sigma_2 \geq \dots \geq \sigma_{\min\{m,n\}}$ be the singular values. Suppose that the following conditions hold:*

1° $\sigma(\mathbf{L}_k)$, $\sigma(\mathbf{R}_k)$ are uniformly bounded.

2° $\mathcal{R}(\mathbf{L})_0$ is in a neighborhood of the exact solution.

Then Algorithm 3 is local q -linear convergent, and the convergence ratio is approximately $\sigma_{r+1}^2/\sigma_r^2$, where $\sigma_{r+1} < \sigma_r$.

This theorem illustrates the convergence of the ALS method in a viewpoint of subspace, and the convergence ratio depends on the gap of σ_r and σ_{r+1} . The detailed proof can be found in Appendix A.

Remark 1 *If condition 1° in Theorem 1 is not satisfied, then either \mathbf{L}_k or \mathbf{R}_k is close to singular. This implies that the truncation r is inappropriately chosen, i.e., greater than the numerical rank of \mathbf{A} .*

An evaluation of the convergence region of the ALS method can be found in the following theorem.

Theorem 2 *Under the assumption of Theorem 1, provided that the initial guess \mathbf{L}_0 satisfies*

$$\|\mathbf{L}_0^{(2)} \mathbf{L}_0^{(1)-1}\|_2 \leq \sqrt{\frac{\sigma_r^2 - (\sigma_r - \varepsilon)^2}{(\sigma_r - \varepsilon)^2 - \sigma_{\min}^2}}, \quad (3.1)$$

then the ALS method converges to the exact solution. Here

$$\mathbf{U}^T \mathbf{L}_0 = \begin{pmatrix} \mathbf{U}_1^T \mathbf{L}_0 \\ \mathbf{U}_2^T \mathbf{L}_0 \end{pmatrix} = \begin{pmatrix} \mathbf{L}_0^{(1)} \\ \mathbf{L}_0^{(2)} \end{pmatrix},$$

$\mathbf{A} = \mathbf{U} \mathbf{\Sigma} \mathbf{V}^T$ is the full SVD of \mathbf{A} , $\mathbf{U} = [\mathbf{U}_1, \mathbf{U}_2]$ is the block form of \mathbf{U} , and ε is an arbitrary positive number such that

$$\sigma_r - \varepsilon > \sigma_{r+1}.$$

The proof of Theorem 2 can be found in Appendix B. We remark that it can be seen from the theorem that, within the convergence region, better initial guess is guaranteed to lead to faster convergence. It is also worth noting that (3.1) indicates that the convergence region depends on ε . A smaller ε means higher requirement for the initial guess, but less number of iterations.

With the help of Algorithm 3, we are able to solve the rank- R_n approximation problem to obtain the dominant subspace of $\mathbf{A}_{(n)}$ in t -HOSVD. Based on it, we derive the ALS accelerated versions of the t -HOSVD algorithm, namely t -HOSVD-ALS, presented in Algorithm 4.

Algorithm 4 t -HOSVD-ALS

Input: Tensor $\mathbf{A} \in \mathbb{R}^{I_1 \times I_2 \times \dots \times I_N}$, truncation (R_1, R_2, \dots, R_N)

Output: Low multilinear rank approximation $\hat{\mathbf{A}} \approx \mathbf{G} \times_1 \mathbf{U}^{(1)} \times_2 \mathbf{U}^{(2)} \dots \times_N \mathbf{U}^{(N)}$

- 1: **for all** $n \in \{1, 2, \dots, N\}$ **do**
 - 2: $[\mathbf{L}, \sim] = \text{ALS}(\mathbf{A}_{(n)}, R_n)$
 - 3: Reduced QR decomposition $\mathbf{L} = \hat{\mathbf{Q}}\hat{\mathbf{R}}$
 - 4: $\mathbf{U}^{(n)} = \hat{\mathbf{Q}}$
 - 5: **end for**
 - 6: $\mathbf{G} = \mathbf{A} \times_1 \mathbf{U}^{(1)T} \times_2 \mathbf{U}^{(2)T} \dots \times_N \mathbf{U}^{(N)T}$
-

The ALS improved t -HOSVD algorithm, referred to as st -HOSVD-ALS can be analogously derived, as presented in Algorithm 5.

Algorithm 5 st -HOSVD-ALS

Input: Tensor $\mathbf{A} \in \mathbb{R}^{I_1 \times I_2 \times \dots \times I_N}$, truncation (R_1, R_2, \dots, R_N)

Output: Low multilinear rank approximation $\hat{\mathbf{A}} \approx \mathbf{G} \times_1 \mathbf{U}^{(1)} \times_2 \mathbf{U}^{(2)} \dots \times_N \mathbf{U}^{(N)}$

- 1: Select an order of $\{1, 2, \dots, N\}$, i.e., $\{i_1, i_2, \dots, i_N\}$
 - 2: Let $\mathbf{B} = \mathbf{A}$
 - 3: **for all** $n \in \{i_1, i_2, \dots, i_N\}$ **do**
 - 4: Mode- n matricization $\mathbf{B}_{(n)} \leftarrow \mathbf{B}$
 - 5: $[\mathbf{L}, \mathbf{R}] = \text{ALS}(\mathbf{B}_{(n)}, R_n)$
 - 6: Reduced QR decomposition $\mathbf{L} = \hat{\mathbf{Q}}\hat{\mathbf{R}}$
 - 7: $\mathbf{U}^{(n)} = \hat{\mathbf{Q}}$
 - 8: Update $\mathbf{B}_{(n)} = \hat{\mathbf{R}}\mathbf{R}^T$
 - 9: $\mathbf{B} \leftarrow \mathbf{B}_{(n)}$ in tensor format
 - 10: **end for**
 - 11: $\mathbf{G}_{(i_N)} = \mathbf{B}_{(i_N)}$
 - $\mathbf{G} \leftarrow \mathbf{G}_{(i_N)}$ in tensor format
-

The difference between Algorithm 4 and 5 is whether or not to store \mathbf{R} and $\hat{\mathbf{R}}$, the right factor matrices of the ALS method and reduced QR decomposition, respectively. Storing them will help reduce the overall computational cost when updating tensor \mathbf{B} , and core tensor \mathbf{G} can be calculated with the last factor matrix simultaneously in Algorithm 5. Apart from the computational cost of

ALS in the t -HOSVD-ALS algorithm, calculating the core tensor \mathcal{G} is also critical, especially for higher-order tensors. An extra advantage of the st -HOSVD-ALS is that the computational cost of core tensor is avoided as much as possible.

Compared with t -HOSVD and st -HOSVD, the proposed algorithms exhibit several advantages. First, the redundant computations of the singular vectors are totally avoided, thus the overall cost of the algorithm can be substantially reduced. Second, the convergence of the ALS procedure is controllable by adjusting the convergence tolerance. This is helpful considering the fact that t -HOSVD and st -HOSVD are quasi-optimal, and are often used as the initial guess for other iterative algorithms such as HOOI. Third, the algorithms are free of intermediate data explosion since the least square problems can be solved without explicitly computing $\mathbf{A}_{(n)}$ or $\mathbf{B}_{(n)}$.

An added benefit of the proposed t -HOSVD-ALS and st -HOSVD-ALS algorithms is that the solution of the multi-side least squares problems is intrinsically parallelizable. By using the ALS method, each row of the factor matrix \mathbf{L} or \mathbf{R} can be independently updated. Therefore, one can distribute the computation of the rows over multiple computing units. Since the workload for each row is almost identical, a simple static load distribution strategy suffices. All other operations in the algorithms, such as the matrix-matrix multiplication, the QR reduction and the matrix inversion, can also be easily parallelized by calling vendor-supplied highly optimized linear algebra libraries.

4 Computational Cost and Error Analysis

In the proposed t -HOSVD-ALS and st -HOSVD-ALS algorithms, the performance of the ALS iteration depends on several factors, such as the initial guess and the convergence criterion. Based on the convergence property and the convergence condition of the ALS method, we suggest to set the initial guess \mathbf{L}_0 as follows.

1. Generate a random matrix \mathbf{S} , whose entries are uniform distributions on interval $[0, 1]$.
2. Compute the reduced QR decomposition $\mathbf{A}_{(n)}\mathbf{S} = \mathbf{Q}\mathbf{R}$.
3. Let \mathbf{Q} be the initial guess, i.e., $\mathbf{L}_0 = \mathbf{Q}$.

In this way, it is assured that $\mathcal{R}(\mathbf{L}_0)$ is a subspace of $\mathcal{R}(\mathbf{A}_{(n)})$, which is closer to the left dominant subspace of $\mathbf{A}_{(n)}$ than a random initial guess. Also, step 3 makes sure that the initial guess is properly normalized.

The stopping condition of the ALS iteration can be set to

$$|\|\mathbf{A}_{(n)} - \mathbf{L}_k \mathbf{R}_k^T\|_F - \|\mathbf{A}_{(n)} - \mathbf{U}_1 \mathbf{U}_1^T \mathbf{A}_{(n)}\|_F| \leq \eta \|\mathbf{A}\|_F, \quad (4.1)$$

where $\mathcal{R}(\mathbf{U}_1)$ is the left dominant subspace of $\mathbf{A}_{(n)}$, and η is an accuracy tolerance parameter. In practice, however, \mathbf{U}_1 is often not available. We therefore advise to replace (4.1) by

$$|\|\mathbf{A}_{(n)} - \mathbf{L}_k \mathbf{R}_k^T\|_F - \|\mathbf{A}_{(n)} - \mathbf{L}_{k+1} \mathbf{R}_{k+1}^T\|_F| \leq \eta \|\mathbf{A}\|_F \quad (4.2)$$

as the stop criterion.

Next, we will discuss truncation R_n and how to select the tolerance parameter η by error analysis. To analyze the approximation error of ALS-based algorithms, we first recall a useful lemma.

Lemma 2 [56] *Let $\mathbf{U}^{(n)} \in \mathbb{R}^{I_n \times R_n}$, $n \in \{1, 2, \dots, N\}$ be a sequence of column orthogonal matrices, calculated via the t -HOSVD or st -HOSVD algorithm, and suppose that $\hat{\mathcal{A}} = \mathcal{A} \times_1 (\mathbf{U}^{(1)} \mathbf{U}^{(1)T}) \times_2$*

$(\mathbf{U}^{(2)}\mathbf{U}^{(2)T}) \dots \times_N (\mathbf{U}^{(N)}\mathbf{U}^{(N)T})$ is an approximation of $\mathcal{A} \in \mathbb{R}^{I_1 \times I_2 \times \dots \times I_N}$. Then

$$\|\hat{\mathcal{A}} - \mathcal{A}\|_F^2 \leq \sum_{n=1}^N \gamma_n \leq N \|\mathcal{A} - \mathcal{A}_{opt}\|_F^2, \quad (4.3)$$

where $\gamma_n = \sum_{r=R_n+1}^{I_n} (\sigma_r^{(n)})^2$, and \mathcal{A}_{opt} is the optimal solution of problem (1.1).

It is worth noting that although estimation (4.3) ignores the computation error, it is still useful in practice. By Lemma 2, the error analysis of our algorithms is described in Theorem 3, with proof given in Appendix C.

Theorem 3 *If the stop criterion of ALS is set to (4.1), then the approximation errors of Algorithm 4 and 5 are bounded by*

$$\frac{\|\hat{\mathcal{A}} - \mathcal{A}\|_F}{\|\mathcal{A}\|_F} \leq \sqrt{\sum_{n=1}^N (\eta_n^2 + \frac{\gamma_n}{\|\mathcal{A}\|_F^2})} \leq \sqrt{N}(\eta + \frac{\|\mathcal{A} - \mathcal{A}_{opt}\|_F}{\|\mathcal{A}\|_F}), \quad (4.4)$$

where $\eta = \max_{n \in \{1, 2, \dots, N\}} \eta_n$.

We remark that although in practice (4.1) is replaced by (4.2), numerical tests indicate that the main result (4.4) still holds. From (4.4), we advice to choose the tolerance parameter η_n such that the dominant term in the right hand side of (4.4) is $\gamma_n/\|\mathcal{A}\|_F^2$ or $\|\mathcal{A} - \mathcal{A}_{opt}\|_F/\|\mathcal{A}\|_F$. Furthermore, if truncation R_n is selected appropriately, both γ_n and η_n will be small, and the ALS will converge very fast since $\sigma_{R_n+1}/\sigma_{R_n} \ll 1$. On the other hand, less suitable truncation R_n represents larger γ_n and therefore larger η_n , which in turn reduces the required number of ALS iterations.

Also of interest to us is the overall costs of the proposed algorithms. We analyze cases related to both general higher-order tensor $\mathcal{A} \in \mathbb{R}^{I_1 \times I_2 \times \dots \times I_N}$ with truncation (R_1, R_2, \dots, R_N) and cubic tensor $\mathcal{A} \in \mathbb{R}^{I \times I \times I \times \dots \times I}$ with truncation (R, R, \dots, R) . The computational complexities of the t -HOSVD-ALS and st -HOSVD-ALS algorithms are listed in Table 1, where iter_n is the number of ALS iterations for mode n .

Table 1: Computational cost of our algorithms

Algorithm	$\mathcal{A} \in \mathbb{R}^{I_1 \times I_2 \times \dots \times I_N}$	$\mathcal{A} \in \mathbb{R}^{I \times I \times \dots \times I}$
t -HOSVD-ALS	$\mathcal{O}(\sum_{n=1}^N (R_n I_{1:N}) \text{iter}_n)$	$\mathcal{O}(\sum_{n=1}^N (R I^N) \text{iter}_n)$
st -HOSVD-ALS	$\mathcal{O}(\sum_{n=1}^N (R_n I_{n:N}) \text{iter}_n)$	$\mathcal{O}(\sum_{n=1}^N (R I^{N-n+1}) \text{iter}_n)$

From the table we can see that the computational costs rely greatly on iter_n , which in turn depends on the initial guess, the truncation R_n and the accuracy requirement. Our numerical results reveal that iter_n is usually far smaller than R_n , indicating the low computational costs of the proposed algorithms.

5 Numerical Experiments

In this section, we will compare the proposed ALS-based algorithms with the original t -HOSVD and st -HOSVD algorithms by several numerical experiments related to both synthetic and real-world tensors. The implementation of the original algorithms includes $t(st)$ -HOSVD-svds which uses matrix SVD to calculate the leading left singular vectors of matrix and $t(st)$ -HOSVD-eigs which uses eigen-decomposition of the Gram matrix instead. To examine the numerical behaviors of these algorithms, we carry out most the experiments in MATLAB v2017b on a laptop computer equipped with an Intel Core i5-8250U CPU of 1.60 GHz. And to study the parallel performance of the proposed algorithms, we implement the algorithms in C and run them on a workstation equipped with an 32-core Intel Xeon E5-2620 CPU of 2.10 GHz. Unless mentioned otherwise, the tolerance parameter is set to $\eta = 10^{-4}$, and the maximum number of ALS iterations is limited to 1,000 in all tests.

5.1 Reconstruction of random low-rank tensors with noise

In the first set of experiments we examine the performance of the original truncated HOSVD algorithms and the proposed ALS-based ones for the reconstruction of random low-rank tensors with noise. The tests are designed following the work of Zhang and Golub [64]. Specifically, the input tensor is randomly generated as

$$\hat{\mathcal{A}} = \mathcal{A} + \delta \mathcal{E},$$

where the elements of \mathcal{E} follow the standard Gaussian distribution, and the noisy level is controlled by $\delta = 10^{-2}$. The base tensor $\mathcal{A} \in \mathbb{R}^{I \times I \times I}$ has a low multilinear rank structure, which is constructed by

$$\mathcal{A} = \lambda_1 \cdot \mathbf{a}_1 \circ \mathbf{b}_1 \circ \mathbf{c}_1 + \lambda_2 \cdot \mathbf{a}_2 \circ \mathbf{b}_2 \circ \mathbf{c}_2 + \cdots + \lambda_R \cdot \mathbf{a}_R \circ \mathbf{b}_R \circ \mathbf{c}_R,$$

where $\mathbf{a}_r, \mathbf{b}_r, \mathbf{c}_r \in \mathbb{R}^I$ are randomly generated normalized vectors, and coefficients $\lambda_r \in [5, 10]$ for all $r \in \{1, 2, \dots, R\}$.

In the tests, we gradually increase the tensor size I from 20 to 280 with step 20 and set the truncation $R = 0.2I$. We carry out the tests for 20 times and draw the averaged reconstruction errors and running time in Fig. 1. From the figure, it is observed that there is almost no difference in reconstruction error among all tested algorithms, indicating that the proposed ALS-based methods can maintain the accuracy of the original ones. In terms of the running time, t -HOSVD-ALS is $2.4\times \sim 32\times$ faster than t -HOSVD-svds, although not significantly faster than t -HOSVD-eigs. For st -HOSVD the performance improvement from the ALS-based method is much higher. In particular, by using st -HOSVD-ALS, a speedup of $58.1\times \sim 212\times$ and $8.4\times \sim 17.6\times$ is achieved as compared to st -HOSVD-svds and st -HOSVD-eigs, respectively.

5.2 Approximation of sparse random tensors

The second set of experiments is designed for testing the capability of the original truncated HOSVD algorithms and the proposed ALS-based ones on approximating randomly generated sparse

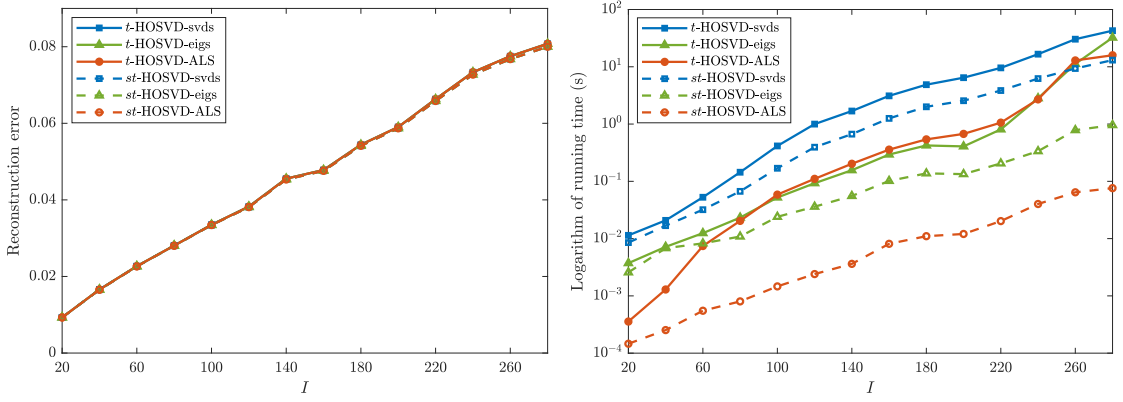


Fig. 1: Reconstruction errors and running time of various truncated HOSVD algorithms for reconstructing random noisy low-rank tensors with gradually increased size.

tensors. Inspired by [39], we set the input fourth-order sparse tensor $\mathcal{A} \in \mathbb{R}^{100 \times 100 \times 100 \times 100}$ to be

$$\mathcal{A} = \sum_{i=1}^{10} \frac{\gamma}{i} \cdot \mathbf{a}_i \circ \mathbf{b}_i \circ \mathbf{c}_i \circ \mathbf{d}_i + \sum_{i=11}^{100} \frac{1}{i^2} \cdot \mathbf{a}_i \circ \mathbf{b}_i \circ \mathbf{c}_i \circ \mathbf{d}_i,$$

where $\gamma = 10$ is an adjustable parameter, $\{\mathbf{a}_i, \mathbf{b}_i, \mathbf{c}_i, \mathbf{d}_i\}$ are sparse unit vectors for all $i \in \{1, 2, \dots, 100\}$, randomly generated with 5% nonzeros.

Considering that the input tensor is sparse, it would be of interest to investigate how different algorithms work with small truncation. We therefore carry out the experiments with the truncation (R, R, R, R) set to $R = 5, 10, 15, 20$, respectively. We run the test for 20 times and record the averaged relative residuals and running time of the tested algorithms in Table 2. We can see from the table that relative residuals of all tested algorithms are almost indistinguishable, which again validates the accuracy of the proposed methods. Table 2 also shows that the original svds-based algorithms are the slowest across all tests. For t -HOSVD, the ALS-based method does not show much advantage in terms of running time as compared with the eigs-based one, especially when the truncation is very small. But for st -HOSVD, the ALS-based approach is substantially faster, cutting the running time by $41.3 \times \sim 933 \times$ as compared with the original eigs-based algorithm.

To further investigate the performance of the proposed ALS-based algorithms, we show the averaged numbers of ALS iterations in Fig. 2, in which iter_n represents the number of ALS iterations for mode n . Overall it can be seen that the required numbers of ALS iterations are quite low. Especially for all cases with $R \geq 10$, only around 4 iterations are needed for the ALS iteration to converge. The reason behind this interesting observation is that by construction of the tensor \mathcal{A} , the gap of singular values σ_R and σ_{R+1} is large when $R \geq 10$ but small otherwise. This is consistent with our previous theoretical analysis on the convergence behavior of the ALS method.

5.3 Compression tensors arising from fluid dynamics simulations

The purpose of this set of experiments is to examine the performance of different truncated HOSVD algorithms for compressing tensors generated from the simulation results of a lid-driven

Algorithm		t -HOSVD			st -HOSVD		
		svds	eigs	ALS	svds	eigs	ALS
$R = 5$	relative residual ($\times 10^{-1}$)	2.5569	2.5569	2.5591	2.4242	2.4242	2.4257
	running time (s)	14.74	4.25	6.88	3.51	0.84	0.0009
$R = 10$	relative residual ($\times 10^{-3}$)	1.3592	1.3592	1.3592	1.3592	1.3592	1.3592
	running time (s)	26.56	4.12	3.03	7.08	0.87	0.001
$R = 15$	relative residual ($\times 10^{-4}$)	7.8033	7.8033	8.5311	7.5960	7.5960	8.0237
	running time (s)	42.69	4.81	4.14	11.91	1.00	0.01
$R = 20$	relative residual ($\times 10^{-4}$)	5.4019	5.4019	5.6548	5.0365	5.0365	5.3724
	running time (s)	66.17	6.71	5.32	18.45	1.24	0.03

Table 2: Relative residuals and running time of various truncated HOSVD algorithms for approximating sparse random tensors with different truncations.

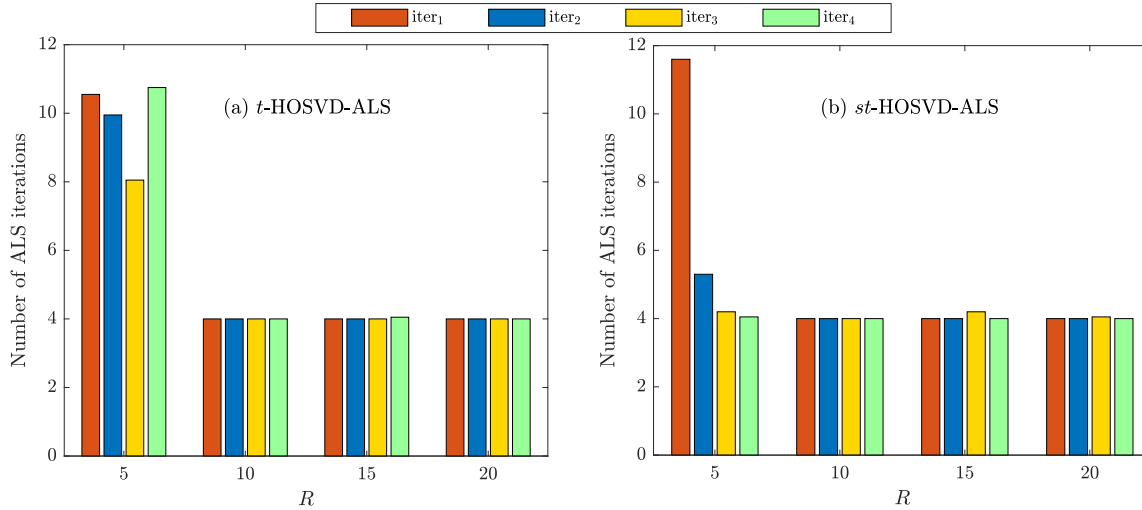


Fig. 2: Number of ALS iterations in the proposed ALS-based methods for approximating sparse random tensors with different truncations.

cavity flow, which is a standard benchmark for incompressible fluid dynamics [10]. The simulation is done in a square domain of length 1 m with the speed of the top plate setting to 1 m/s and all other boundaries no flip. The kinematic viscosity is $\nu = 1.0 \times 10^{-4}$ m²/s, and the fluid properties is assumed to be laminar. We use the OpenFOAM software package [2] to conduct the simulation on a uniform grid with 512 grid cells in each direction. The simulation is run with time step $\Delta t = 2.0 \times 10^{-4}$ s and terminated at $t = 1.0$ s. We record the magnitude of velocity at $t = 0.01$ s, 0.02 s, \dots , 1.0 s. The simulation results of the lid-driven cavity flow are stored in a third-order tensor of size $512 \times 512 \times 100$. To test the tensor approximation algorithms, we fix the truncation to (64, 64, 20), corresponding to a compression ratio of 320 : 1.

Algorithm		<i>t</i> -HOSVD			<i>st</i> -HOSVD		
		svds	eigs	ALS	svds	eigs	ALS
$\eta = 10^{-2}$	relative residual ($\times 10^{-3}$)	1.1240	1.1240	1.1608	1.1240	1.1240	1.1871
	running time (s)	24.10	1.24	0.73	11.30	0.45	0.006
$\eta = 10^{-4}$	relative residual ($\times 10^{-3}$)	1.1240	1.1240	1.1396	1.1240	1.1240	1.1454
	running time (s)	25.02	1.62	1.30	11.83	0.58	0.01
$\eta = 10^{-6}$	relative residual ($\times 10^{-3}$)	1.1240	1.1240	1.1240	1.1240	1.1240	1.1243
	running time (s)	25.19	1.44	2.19	11.54	0.56	0.03

Table 3: Relative residuals and running time of various truncated HOSVD algorithms for compressing tensors arising from fluid dynamics simulations with different tolerance parameters.

First, we study the efficiency of tested algorithms under different accuracy requirements. We run the test for 20 times with tolerance parameter η adjusted to different values and record the averaged relative residual and running time for each value of η ; the test results are listed in Table 3. From the table we have the following observations.

- The relative residuals and running time of the original HOSVD algorithms are insensitive to the change of the tolerance parameter η . This is due to the usage of Krylov subspace method for computing matrix truncated SVD or eigen-decomposition.
- For the ALS-based methods, the relative residuals and the running time both depend on η . With η decreased, the relative residuals are reduced to a similar level that the original HOSVD can attain but more running time is required.
- The svds-based algorithms are the slowest in all tests. *t*-HOSVD-ALS is slightly faster than *t*-HOSVD-eigs when $\eta = 10^{-2}$ and 10^{-4} but the advantage is lost when $\eta = 10^{-6}$. The *st*-HOSVD-ALS method, on the other hand, is substantially faster than *st*-HOSVD-eigs, with a speedup of around $18.7\times \sim 384.7\times$.

It seems from the tests that despite the excellent performance of the proposed *st*-HOSVD-ALS method, the proposed *t*-HOSVD-ALS algorithm is not quite advantageous, especially when the tolerance parameter η is small. In practice an HOSVD algorithm is often used as the initial guess of a supposedly more accurate iterative method such as HOOI. In this case it is not necessary to use a tight tolerance parameter. To examine whether $\eta = 10^{-4}$ is a suitable choice for the ALS-based algorithms in the same tests, we draw in Fig. 3 the contours of the original and compressed velocity data at $t = 0.51$ s. It clearly shows that when $\eta = 10^{-4}$, the compressed results are consistent with each other with no distinguishable difference. In fact, the measured maximum difference between the compressed data obtained by the original *t*-HOSVD and that by *t*-HOSVD-ALS is around 1.25×10^{-4} which is nearly one order of magnitude smaller than the measured compression error, which is around 1.12×10^{-3} in this case.

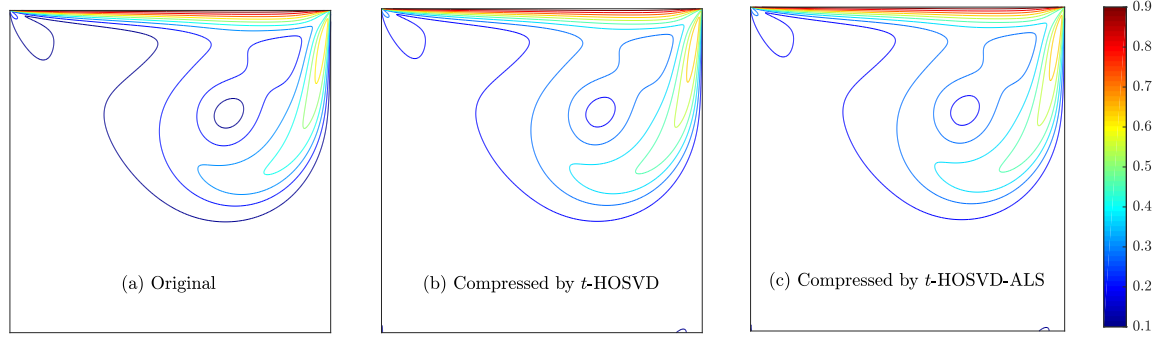


Fig. 3: The original and compressed data at $t = 0.51$ s for compressing tensors arising from fluid dynamics simulations with tolerance parameter $\eta = 10^{-4}$.

To further investigate the applicability of the compressed results, we use the computed truncated HOSVD with tolerance parameter $\eta = 10^{-4}$ as the initial guess of the HOOI method with stopping criterion 10^{-12} . The HOOI method is taken from the MATLAB Tensor Toolbox v3.1 [5]. The test results are presented in Table 4, in which we list the relative residuals with the HOSVD provided initial guesses, the final relative residuals of HOOI, and the number of HOOI iterations, all averaged on 20 independent runs. From the table we can see that although the initial residual provided by the ALS-based algorithms are slightly larger than those provided by the original truncated HOSVD methods, same final residuals can be achieved after HOOI iterations nevertheless. And more importantly, the required numbers of HOOI iterations are insensitive to which specific HOSVD algorithms, original or not, are used as shown in the tests. In other words, the proposed ALS-based methods are able to deliver similar results as the original ones when applying in HOOI, even when the tolerance parameter is relatively loose.

Algorithm	Relative residual		Number of HOOI iterations
	Initial	Final	
t -HOSVD-svds	1.1240×10^{-3}	1.1209×10^{-3}	5.0
t -HOSVD-eigs	1.1240×10^{-3}	1.1209×10^{-3}	5.0
t -HOSVD-ALS	1.1396×10^{-3}	1.1209×10^{-3}	5.5
st -HOSVD-svds	1.1240×10^{-3}	1.1209×10^{-3}	6.0
st -HOSVD-eigs	1.1240×10^{-3}	1.1209×10^{-3}	6.0
st -HOSVD-ALS	1.1454×10^{-3}	1.1209×10^{-3}	6.0

Table 4: A comparison of HOOI results for compressing tensors arising from fluid dynamics simulations with initial solutions provided by various truncated HOSVD algorithms.

5.4 Parallel performance

An advantage of the proposed ALS-based methods is that they are easy to parallelize. In this experiment, we implement the t -HOSVD-ALS and st -HOSVD-ALS algorithms in C++ with OpenMP multi-threading parallelization [3]. The involved linear algebra operations are available with parallelization from the Intel MKL [1, 59] and the open-source ARMADILLO [45, 46] libraries. In the test we choose the input tensor to be the randomly generated ones in the first set of experiments and set the size of the tensor to be $400 \times 400 \times 400$ and the truncation to be $R = 80$. We break down the running time into different portions, including the ALS iterations along the three dimensions (ALS- i , $i \in \{1, 2, 3\}$) and the calculation of the core tensor. The test results are drawn in Fig. 4. Also shown in the figure is the parallel scalability of the proposed algorithms.

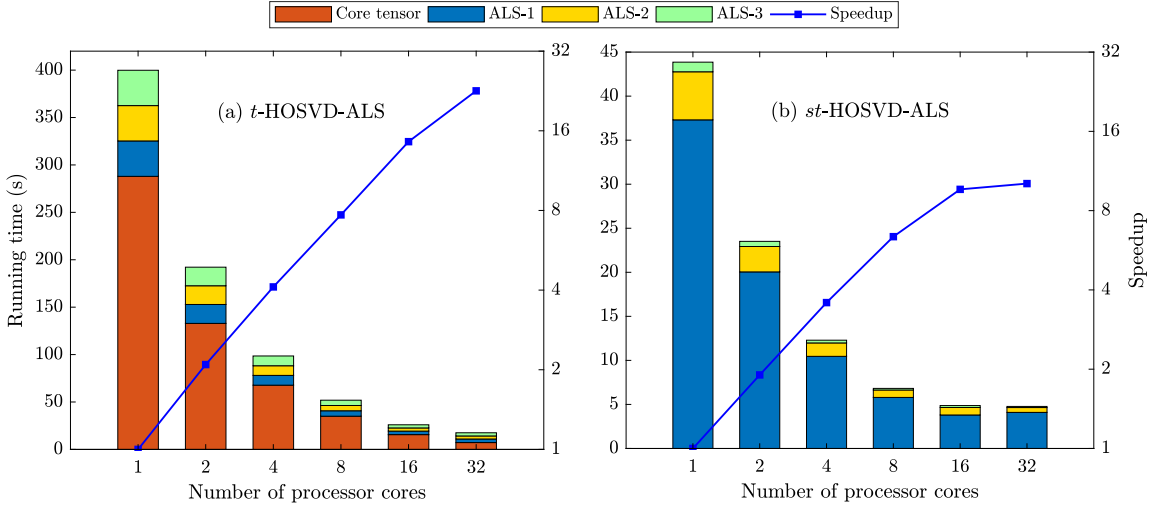


Fig. 4: The running time and speedup of the ALS-based truncated HOSVD algorithms for reconstructing random noisy low-rank tensors on a parallel computer.

From Fig. 4(a), one can observe that t -HOSVD-ALS is highly scalable. A speedup of $22.7\times$ can be achieved when the number of processor cores is increased from 1 to 32, corresponding to a parallel efficiency of 70.9%. In particular, major operations of the t -HOSVD-ALS, including ALS iterations and core tensor calculations, are all accelerated efficiently with the increased number of processor cores. On the other hand, it can be seen from Fig. 4(b) that st -HOSVD-ALS can also achieve satisfactory parallel scalability of $9.6\times$ when the number of processor cores is increased from 1 to 16, corresponding to a parallel efficiency of 60.0%. There is a drop of parallel efficiency when using 32 processor cores, this is expected considering the fact that the st -HOSVD-ALS algorithm is nearly an order of magnitude faster than t -HOSVD-ALS as tested, therefore the running time with 32 processor cores is too short, not able to compensate the parallelization overhead. Another interesting observation one can make is that in st -HOSVD-ALS the calculation of core tensor no longer plays a role. Instead, the ALS along different dimensions are the major cost. Overall, the test results clearly show that the proposed ALS-based algorithms can be easily scalable with high parallel efficiency.

6 Conclusions

In this paper, we proposed a class of ALS-based algorithms for solving the truncated HOSVD problem. Compared with the original t -HOSVD and st -HOSVD algorithms, the proposed algorithms are superior in several ways. First, by eliminating the redundant computations of the singular vectors, the overall costs of the algorithms are substantially reduced. Second, the proposed algorithms are more flexible with adjustable convergence tolerance, which is especially useful when the algorithms are used to generate initial solutions for iterative methods such as HOOI. Third, the proposed algorithms are free of the notorious data explosion issue due to the fact that the ALS procedure does not explicitly require the intermediate matrices. And fourth, the ALS-based approaches are parallelization friendly on high-performance computers. Theoretical analysis shows that the ALS iteration in the proposed algorithms is q -linear convergent with a relatively wide convergence region. Numerical experiments with both synthetic and real-world tensor data demonstrate that proposed ALS-based algorithms can substantially reduce the total cost of truncated HOSVD and are highly parallelizable.

Possible future works could include applying of the proposed ALS-based algorithms to more applications, among which we are especially interest in large-scale scientific computing. It would also be of interest to study randomization techniques to further improve the performance of the proposed algorithms, considering the fact that solving multiple least squares problems with different right-hand sides is the major cost. Some of the ideas presented in this work, such as the utilization of ALS for solving the intermediate low rank approximation problem, might be possible to extend to other tensor decomposition models such as tensor-train (TT) and hierarchical Tucker (HT) decompositions.

References

1. Intel Math Kernel Library Reference Manual [EQ/OL]. URL <http://developer.intel.com>
2. OpenFoam 2018, Version 6. URL <https://openfoam.org>
3. OpenMP application program interface, Version 4.0, OpenMP Architecture Review Board (July, 2013). URL <http://www.openmp.org>
4. Austin, W., Ballard, G., Kolda, T.G.: Parallel tensor compression for large-scale scientific data. In: IEEE International Parallel and Distributed Processing Symposium, pp. 912–922. IEEE (2016)
5. Bader, B.W., Kolda, T.G., et.al.: MATLAB Tensor Toolbox Version 3.1. Available online (2019). URL <https://www.tensor toolbox.org>
6. Baglama, J., Reichel, L.: Augmented implicitly restarted Lanczos bidiagonalization methods. SIAM J. Sci. Comput. **27**(1), 19–42 (2005)
7. Beckmann, C., Smith, S.: Tensorial extensions of independent component analysis for multisubject fMRI analysis. Neuroimage **25**(1), 294–311 (2005)
8. Beylkin, G., Mohlenkamp, M.J.: Numerical operator calculus in higher dimensions. Proc. Natl. Acad. Sci. **99**, 10246–10251 (2002)
9. Bro, R.: Review on multiway analysis in chemistry 2000/2005. Crit. Rev. Anal. Chem. **36**, 279–293 (2006)
10. Burggraf, R.: Analytical and numerical studies of the structure of steady separated flows. J. Fluid Mechanics **24**(1), 113–151 (1966)
11. Carroll, J.D., Chang, J.J.: Analysis of individual differences in multidimensional scaling via an N -way generalization of Eckart-Young decomposition. Psychometrika **35**, 283–319 (1970)
12. Charalampous, K., Gasteratos, A.: A tensor-based deep learning framework. Image and Vision Computing **32**(11), 916–929 (2014)
13. Cullum, J., Willoughby, R., Lake, M.: A Lanczos algorithm for computing singular values and vectors of large matrices. SIAM J. Sci. Stat. Comput. **4**(2), 197–215 (1983)
14. De Lathauwer, L., De Moor, B., Vandewalle, J.: A multilinear singular value decomposition. SIAM J. Matrix Anal. Appl. **21**(4), 1253–1278 (2000)

15. De Lathauwer, L., De Moor, B., Vandewalle, J.: On the best rank-1 and rank- (r_1, r_2, \dots, r_N) approximation of higher-order tensors. *SIAM J. Matrix Anal. Appl.* **21**, 1324–1342 (2000)
16. De Lathauwer, L., Vandewalle, J.: Dimensionality reduction in higher-order signal processing and rank- (r_1, r_2, \dots, r_N) reduction in multilinear algebra. *Linear Algebra Appl.* **391**, 31–55 (2004)
17. De Leeuw, J., Young, F., Takane, Y.: Additive structure in qualitative data: An alternating least squares method with optimal scaling features. *Psychometrika* **41**, 471–503 (1976)
18. De Silva, V., Lim, L.H.: Tensor rank and the ill-posedness of the best low-rank approximation problem. *SIAM J. Matrix Anal. Appl.* **30**(3), 1084–1127 (2008)
19. Ding, W., Wei, Y.: Solving multi-linear systems with \mathcal{M} -tensors. *J. Sci. Comput.* **68**, 689–715 (2016)
20. Elden, L., Savas, B.: A Newton-Grassmann method for computing the best multilinear rank- (r_1, r_2, r_3) approximation of a tensor. *SIAM J. Matrix Anal. Appl.* **31**(2), 248–271 (2009)
21. Golub, G.H., Van Loan, C.F.: *Matrix Computations* Ed. 4th. Johns Hopkins University Press, Baltimore (2008)
22. Grasedyck, L.: Hierarchical singular value decomposition of tensors. *SIAM J. Matrix Anal. Appl.* **31**(4), 2029–2054 (2010)
23. Hackbusch, W.: Numerical tensor calculus. *Acta Numerica* **23**, 651–742 (2014)
24. Hackbusch, W., Kühn, S.: A new scheme for the tensor representation. *J. Fourier Anal. Appl.* **15**, 706–722 (2009)
25. Henrion, R.: Body diagonalization of core matrices in three-way principal components analysis: Theoretical bounds and simulation. *J. Chemometrics* **7**, 477494 (1993)
26. Hitchcock, F.L.: Multiple invariants and generalized rank of a p -way matrix or tensor. *J. Math. Phys.* **7**(1-4), 39–79 (1928)
27. Holtz, S., Rohwedder, T., Schneider, R.: The alternating linear scheme for tensor optimization in the tensor train format. *SIAM J. Sci. Comput.* **34**(2), A683–A713 (2012)
28. Ishteva, M., Absil, P.A., Van Huffel, S., De Lathauwer, L.: Best low multilinear rank approximation of higher-order tensors, based on the Riemannian trust-region scheme. *SIAM J. Matrix Anal. Appl.* **31**(1), 115–135 (2011)
29. Ishteva, M., De Lathauwer, L., Absil, P.A., Huffel, S.: Dimensionality reduction for higher-order tensors: Algorithms and applications. *Int. J. Pure Appl. Math.* **42**(3), 337–343 (2012)
30. Ishteva, M., De Lathauwer, L., Absil, P.A., Huffel, S.V.: Differential-geometric Newton method for the best rank- (R_1, R_2, R_3) approximation of tensors. *Numer. Algor.* **51**, 179–194 (2009)
31. Jiang, J., Wu, H., Li, Y., Yu, R.: Three-way data resolution by alternating slice-wise diagonalization (ASD) method. *J. Chemometrics* **14**, 15–36 (2000)
32. Khoromskij, B.N.: Tensors-structured numerical methods in scientific computing: Survey on recent advances. *Chemometrics and Intelligent Laboratory Systems* **110**(1), 1–19 (2012)
33. Kiers, H.A.L.: Towards a standardized notation and terminology in multiway analysis. *J. Chemometrics* **14**, 105–122 (2000)
34. Kolda, T.G., Bader, B.W.: Tensor decompositions and applications. *SIAM Rev.* **51**(3), 455–500 (2009)
35. Kroonenberg, P.M.: *Applied Multiway Data Analysis*. John Wiley & Sons. Inc., New Jersey (2008)
36. Kroonenberg, P.M., De Leeuw, J.: Principal component analysis of three-mode data by means of alternating least squares algorithms. *Psychometrika* **45**, 69–97 (1980)
37. Levin, J.: Three-mode factor analysis. Ph.D. thesis, University of Illinois, Urbana-Champaign (1963)
38. Li, J., Battaglino, C., Perros, I., Sun, J., Vuduc, R.: An input-adaptive and in-place approach to dense tensor-times-matrix multiply. In: *Proceedings of the International Conference for High Performance Computing*, 76, pp. 1–12. ACM (2015)
39. Minster, R., Saibaba, A.K., Kilmer, M.E.: Randomized algorithms for low-rank tensor decompositions in the Tucker format. *SIAM J. Math. Data. Sci.* **2**(1), 189–215 (2020)
40. Novikov, A., Podoprikin, D., Osokin, A., Vetrov, D.: Tensorizing neural networks. In: *Annual Conference on Neural Information Processing Systems*, vol. 1, pp. 442–450. ACM (2015)
41. Oh, J., Shin, K., Papalexakis, E., Faloutsos, C., Yu, H.: S-HOT: Scalable high-Order Tucker decomposition. In: *Proceedings of the Tenth ACM International Conference on Web Search and Data Mining*, pp. 761–770. ACM (2017)
42. Oseledets, I.V., Tyrtshnikov, E.E.: Breaking the curse of dimensionality, or how to use SVD in many dimensions. *SIAM J. Sci. Comput.* **31**(5), 3744–3759 (2009)
43. Oseledets, I.V.: Tensor-train decomposition. *SIAM J. Sci. Comput.* **33**(5), 2295–2317 (2011)
44. Rajbhandari, S., Nikam, A., Lai, P.W., Stock, K., Krishnamoorthy, S., Sadayappan, P.: A communication-optimal framework for contracting distributed tensors. In: *Proceedings of the International Conference for High Performance Computing, Networking, Storage and Analysis*, pp. 375–386. IEEE (2014)
45. Sanderson, C., Curtin, R.: Armadillo: A template-based C++ library for linear algebra. *J. Open Source Software* **1**(2), 26 (2016)
46. Sanderson, C., Curtin, R.: A user-friendly hybrid sparse matrix class in C++. In: *International Conference on Mathematical Software, Lecture Notes in Computer Science (LNCS)*, vol. 10931, pp. 422–430. Springer (2018)

47. Savas, B., Lim, L.H.: Quasi-Newton methods on Grassmannians and multilinear approximations of tensors. *SIAM J. Sci. Comput.* **32**(6), 3352–3393 (2009)
48. Schatz, M.: Distributed tensor computations: Formalizing distributions, redistributions, and algorithm derivations. Ph.D. thesis, University of Texas, Austin (2015)
49. Shashua, A., Levin, A.: Linear image coding for regression and classification using the tensor-rank principle. In: *IEEE Conference on Computer Vision and Pattern Recognition*, pp. 42–49. IEEE (2001)
50. Sidiropoulos, N.D., De Lathauwer, L., Xiao, F., Huang, K.J., Papalexakis, E.E., Faloutsos, C.: Tensor decomposition for signal processing and machine learning. *IEEE Trans. on Sig. Proc.* **65**(13), 3551–3582 (2017)
51. Smith, S., Ravindran, N., Sidiropoulos, N., Karpis, G.: Efficient and parallel sparse tensor matrix multiplication. In: *IEEE International Parallel and Distributed Processing Symposium*, pp. 61–70. IEEE (2015)
52. Sorensen, D.: Implicit application of polynomial lters in a k -step Arnoldi method. *SIAM J. Matrix Anal. Appl.* **13**(1), 357–385 (1992)
53. Stewart, G.: A KrylovSchur algorithm for large eigenproblems. *SIAM J. Matrix Anal. Appl.* **23**(3), 601–614 (2001)
54. Szlam, A., Tulloch, A., Tygert, M.: Accurate low-rank approximations via a few iterations of alternating least squares. *SIAM J. Matrix Anal. Appl.* **38**(2), 425–433 (2017)
55. Tucker, L.R.: Some mathematical notes on three-mode factor analysis. *Psychometrika* **31**, 279–311 (1966)
56. Vannieuwenhoven, N., Vandebril, R., Meerbergen, K.: A new truncation strategy for the higher-order singular value decomposition. *SIAM J. Sci. Comput.* **34**(2), A1027–A1052 (2012)
57. Vasilescu, M.A.O., Terzopoulos, D.: Multilinear image analysis for facial recognition. In: *Object recognition supported by user interaction for service robots*, vol. 2, p. 511514. IEEE (2002)
58. Vlasi, D., Brand, M., Pfister, H., Popovic, J.: Face transfer with multilinear models. In: *ACM SIGGRAPH 2005 Papers*, vol. 24, p. 426433. ACM (2005)
59. Wang, E., Zhang, Q., Shen, B., Zhang, G., Lu, X., Wu, Q., Wang, Y.: Intel Math Kernel Library, in *High-Performance Computing on the Intel[®] Xeon Phi*. Springer pp. 167–188 (2014)
60. Wang, S.G., Wu, M.X., Jia, Z.Z.: *Matrix Inequality* Ed. 2th. Science Press, Beijing (2006)
61. Watkins, D.: The QR algorithm revisited. *SIAM Rev.* **50**(1), 133–145 (2008)
62. Xu, Y.: On the convergence of higher-order orthogonal iteration. *Linear and Multilinear Algebra* **66**(11), 2247–2265 (2018)
63. Young, F.W., Takane, Y., De Leeuw, J.: The principal components of mixed measurement level multivariate data: An alternating least squares method with optimal scaling features. *Psychometrika* **43**, 279–281 (1978)
64. Zhang, T., Golub, G.H.: Rank-one approximation to high order tensors. *SIAM J. Matrix Anal. Appl.* **23**(2), 534–550 (2001)

A Proof of Theorem 1

Based on the assumption of Theorem 1, \mathbf{L}_k is nonsingular and $\mathbf{L}_k^T \mathbf{L}_k$ is positive definite. Thus, the iterative form of Algorithm 3 is

$$\begin{aligned} \mathbf{R}_k &= \mathbf{A}^T \mathbf{L}_k (\mathbf{L}_k^T \mathbf{L}_k)^{-1}, \\ \mathbf{L}_{k+1} &= \mathbf{A} \mathbf{R}_k (\mathbf{R}_k^T \mathbf{R}_k)^{-1}, \end{aligned} \tag{A.1}$$

i.e.,

$$\mathbf{L}_{k+1} = \mathbf{A} \mathbf{A}^T \mathbf{L}_k (\mathbf{L}_k^T \mathbf{A} \mathbf{A}^T \mathbf{L}_k)^{-1} (\mathbf{L}_k^T \mathbf{L}_k). \tag{A.2}$$

Suppose that the full SVD of \mathbf{A} is $\mathbf{A} = \mathbf{U} \mathbf{\Sigma} \mathbf{V}^T$, where

$$\mathbf{U} = [\mathbf{U}_1, \mathbf{U}_2], \quad \mathbf{V} = [\mathbf{V}_1, \mathbf{V}_2], \quad \mathbf{\Sigma} = \begin{pmatrix} \mathbf{\Sigma}_1 & 0 \\ 0 & \mathbf{\Sigma}_2 \end{pmatrix}.$$

Then from (A.2), we have

$$\mathbf{U}^T \mathbf{L}_{k+1} = \mathbf{U}^T \mathbf{A} \mathbf{V} \mathbf{V}^T \mathbf{A}^T \mathbf{U} \mathbf{U}^T \mathbf{L}_k (\mathbf{L}_k^T \mathbf{U} \mathbf{U}^T \mathbf{A} \mathbf{V} \mathbf{V}^T \mathbf{A}^T \mathbf{U} \mathbf{U}^T \mathbf{L}_k)^{-1} (\mathbf{L}_k^T \mathbf{U} \mathbf{U}^T \mathbf{L}_k), \tag{A.3}$$

which can be rewritten into block form

$$\begin{pmatrix} \mathbf{L}_{k+1}^{(1)} \\ \mathbf{L}_{k+1}^{(2)} \end{pmatrix} = \begin{pmatrix} \mathbf{\Sigma}_1^2 & 0 \\ 0 & \mathbf{\Sigma}_2 \mathbf{\Sigma}_2^T \end{pmatrix} \begin{pmatrix} \mathbf{L}_k^{(1)} \\ \mathbf{L}_k^{(2)} \end{pmatrix} (\mathbf{L}_k^{(1)T} \mathbf{\Sigma}_1^2 \mathbf{L}_k^{(1)} + \mathbf{L}_k^{(2)T} \mathbf{\Sigma}_2 \mathbf{\Sigma}_2^T \mathbf{L}_k^{(2)})^{-1} (\mathbf{L}_k^{(1)T} \mathbf{L}_k^{(1)} + \mathbf{L}_k^{(2)T} \mathbf{L}_k^{(2)}).$$

It then follows that

$$\begin{aligned}\mathbf{L}_{k+1}^{(1)} &= \boldsymbol{\Sigma}_1^2 \mathbf{L}_k^{(1)} (\mathbf{L}_k^{(1)T} \boldsymbol{\Sigma}_1^2 \mathbf{L}_k^{(1)} + \mathbf{L}_k^{(2)T} \boldsymbol{\Sigma}_2 \boldsymbol{\Sigma}_2^T \mathbf{L}_k^{(2)})^{-1} (\mathbf{L}_k^{(1)T} \mathbf{L}_k^{(1)} + \mathbf{L}_k^{(2)T} \mathbf{L}_k^{(2)}), \\ \mathbf{L}_{k+1}^{(2)} &= \boldsymbol{\Sigma}_2 \boldsymbol{\Sigma}_2^T \mathbf{L}_k^{(2)} (\mathbf{L}_k^{(1)T} \boldsymbol{\Sigma}_1^2 \mathbf{L}_k^{(1)} + \mathbf{L}_k^{(2)T} \boldsymbol{\Sigma}_2 \boldsymbol{\Sigma}_2^T \mathbf{L}_k^{(2)})^{-1} (\mathbf{L}_k^{(1)T} \mathbf{L}_k^{(1)} + \mathbf{L}_k^{(2)T} \mathbf{L}_k^{(2)}).\end{aligned}\tag{A.4}$$

Furthermore,

$$\begin{aligned}& (\mathbf{L}_k^{(1)T} \boldsymbol{\Sigma}_1^2 \mathbf{L}_k^{(1)} + \mathbf{L}_k^{(2)T} \boldsymbol{\Sigma}_2 \boldsymbol{\Sigma}_2^T \mathbf{L}_k^{(2)})^{-1} \\ &= (\mathbf{I} + (\mathbf{L}_k^{(1)T} \boldsymbol{\Sigma}_1^2 \mathbf{L}_k^{(1)})^{-1} (\mathbf{L}_k^{(2)T} \boldsymbol{\Sigma}_2 \boldsymbol{\Sigma}_2^T \mathbf{L}_k^{(2)}))^{-1} (\mathbf{L}_k^{(1)T} \boldsymbol{\Sigma}_1^2 \mathbf{L}_k^{(1)})^{-1} \\ &= (\mathbf{I} + \sum_{n=1}^{\infty} (-1)^n ((\mathbf{L}_k^{(1)T} \boldsymbol{\Sigma}_1^2 \mathbf{L}_k^{(1)})^{-1} (\mathbf{L}_k^{(2)T} \boldsymbol{\Sigma}_2 \boldsymbol{\Sigma}_2^T \mathbf{L}_k^{(2)}))^n) (\mathbf{L}_k^{(1)T} \boldsymbol{\Sigma}_1^2 \mathbf{L}_k^{(1)})^{-1}.\end{aligned}\tag{A.5}$$

Here we suppose that the distance between $\mathcal{R}(\mathbf{L}_k)$ and $\mathcal{R}(\mathbf{U}_2)$ is small enough, therefore can be denoted as δ_k , which only depends on $\|\mathbf{L}_k^{(2)}\|_2$ (i.e., there exist two constants $\alpha, \beta > 0$ such that $\alpha\delta_k \leq \|\mathbf{L}_k^{(2)}\|_2 \leq \beta\delta_k$). We can then obtain the lower bound of the distance between $\mathcal{R}(\mathbf{L}_k)$ and $\mathcal{R}(\mathbf{U}_1)$, which is $\sqrt{1 - \delta_k^2}$, and

$$\|\mathbf{L}_k^{(1)}\|_2 \leq C_1, \quad \|(\mathbf{L}_k^{(1)})^{-1}\|_2 \leq \frac{C_2}{\sqrt{1 - \delta_k^2}},\tag{A.6}$$

where C_1, C_2 are constants independent on k and δ_k . From (A.5) and (A.6), there exists a constant C that is only dependent on C_1, C_2 so that the following inequality holds.

$$(\mathbf{L}_k^{(1)T} \boldsymbol{\Sigma}_1^2 \mathbf{L}_k^{(1)} + \mathbf{L}_k^{(2)T} \boldsymbol{\Sigma}_2 \boldsymbol{\Sigma}_2^T \mathbf{L}_k^{(2)})^{-1} \leq (\mathbf{L}_k^{(1)T} \boldsymbol{\Sigma}_1^2 \mathbf{L}_k^{(1)})^{-1} + \frac{C\delta_k^2}{(1 - 2\delta_k^2)^2},\tag{A.7}$$

Further, from (A.7) and (A.4), assume that $\sigma_r > \sigma_{r+1}$, we have

$$\mathbf{L}_{k+1}^{(2)} \leq \frac{\boldsymbol{\Sigma}_2 \boldsymbol{\Sigma}_2^T}{\sigma_r^2} \mathbf{L}_k^{(2)} (\mathbf{L}_k^{(1)T} \frac{\boldsymbol{\Sigma}_1^2}{\sigma_r^2} \mathbf{L}_k^{(1)})^{-1} (\mathbf{L}_k^{(1)T} \mathbf{L}_k^{(1)}) + \hat{C} \left(\frac{\delta_k^2}{(1 - 2\delta_k^2)^2} + \frac{\delta_k^2}{1 - \delta_k^2} + \frac{\delta_k^4}{(1 - 2\delta_k^2)^2} \right),$$

where \hat{C} is a constant. Clearly,

$$0 < \mathbf{L}_k^{(1)T} \mathbf{L}_k^{(1)} \leq \mathbf{L}_k^{(1)T} \frac{\boldsymbol{\Sigma}_1^2}{\sigma_r^2} \mathbf{L}_k^{(1)},$$

and by Lemma 1, we have

$$\|(\mathbf{L}_k^{(1)T} \frac{\boldsymbol{\Sigma}_1^2}{\sigma_r^2} \mathbf{L}_k^{(1)})^{-1} (\mathbf{L}_k^{(1)T} \mathbf{L}_k^{(1)})\|_2 \leq 1.$$

Since δ_k is small enough, we obtain

$$\|\mathbf{L}_{k+1}^{(2)}\|_2 \leq \frac{\sigma_{r+1}^2}{\sigma_r^2} \|\mathbf{L}_k^{(2)}\|_2 + \tilde{C} \delta_k^2 \leq \frac{\sigma_{r+1}^2}{\sigma_r^2} \|\mathbf{L}_k^{(2)}\|_2 + \frac{\tilde{C}}{\alpha^2} \|\mathbf{L}_k^{(2)}\|_2^2,\tag{A.8}$$

where α, \tilde{C} do not depend on k and $\|\mathbf{L}_k^{(2)}\|_2$.

Denote

$$q = \frac{\sigma_{r+1}^2}{\sigma_r^2} + \frac{\tilde{C}}{\alpha^2} \|\mathbf{L}_0^{(2)}\|_2.$$

Since we assume that $\mathcal{R}(\mathbf{L}_0)$ is close to $\mathcal{R}(\mathbf{U}_1)$ enough, $\|\mathbf{U}_2^T \mathbf{L}_0\|_2$ is sufficiently small, i.e., $\|\mathbf{L}_0^{(2)}\|_2 = o(1)$. In other words, we assume that $q < 1$. From (A.8), we have

$$\|\mathbf{L}_{k+1}^{(2)}\|_2 \leq q \|\mathbf{L}_k^{(2)}\|_2$$

for all k , which leads to

$$\lim_{k \rightarrow +\infty} \|\mathbf{L}_k^{(2)}\|_2 \rightarrow 0.$$

Combining with the assumption of \mathbf{L}_k , it is verified that $\mathcal{R}(\mathbf{L}_k)$ is orthogonal to $\mathcal{R}(\mathbf{U}_2)$ with $k \rightarrow +\infty$. Since the orthogonal complement space of $\mathcal{R}(\mathbf{U}_2)$ is unique, we have

$$\mathcal{R}(\mathbf{L}_k) = \mathcal{R}(\mathbf{U}_1), \quad k \rightarrow +\infty,$$

where $\mathcal{R}(\mathbf{U}_1)$ is the dominant subspace of \mathbf{A} . In other words, we have

$$\lim_{k \rightarrow +\infty} \|\mathbf{L}_k \mathbf{L}_k^\dagger - \mathbf{U}_1 \mathbf{U}_1^T\|_2 = 0,$$

where \mathbf{L}_k^\dagger is the pseudo-inverse of \mathbf{L}_k . Further, from the iterative form of the ALS method, we have

$$\mathbf{R}_k = \mathbf{A}^T (\mathbf{L}_k^\dagger)^T,$$

thus

$$\mathbf{L}_k \mathbf{R}_k^T = \mathbf{L}_k \mathbf{L}_k^\dagger \mathbf{A} \rightarrow \mathbf{U}_1 \mathbf{U}_1^T \mathbf{A}, \quad k \rightarrow +\infty.$$

And since the Frobenius norm $\|\cdot\|_F$ is continuous,

$$\lim_{k \rightarrow +\infty} \|\mathbf{A} - \mathbf{L}_k \mathbf{R}_k^T\|_F = \|\mathbf{A} - \mathbf{U}_1 \mathbf{U}_1^T \mathbf{A}\|_F.$$

Since $\mathbf{U}_1 \mathbf{U}_1^T \mathbf{A}$ is the exact solution of low rank approximation of \mathbf{A} , the convergence of the ALS method is proved.

From (A.8), we further confirm the q -linear convergence of the ALS method, with approximate convergence ratio $\sigma_{r+1}^2 / \sigma_r^2$. \square

B Proof of Theorem 2

The assumption of Theorem 1 implies that \mathbf{L}_k is nonsingular at every iteration k . We assume that

$$\mathbf{L}_k^{(1)T} \boldsymbol{\Sigma}_1^2 \mathbf{L}_k^{(1)} + \mathbf{L}_k^{(2)T} \boldsymbol{\Sigma}_2 \boldsymbol{\Sigma}_2^T \mathbf{L}_k^{(2)}$$

is positive definite. Let ε be a positive number such that $\sigma_r > \sigma_{r+1} - \varepsilon$. By (A.4), we know

$$\begin{aligned} \mathbf{L}_{k+1}^{(1)} &= \boldsymbol{\Sigma}_1^2 \mathbf{L}_k^{(1)} (\mathbf{L}_k^{(1)T} \boldsymbol{\Sigma}_1^2 \mathbf{L}_k^{(1)} + \mathbf{L}_k^{(2)T} \boldsymbol{\Sigma}_2 \boldsymbol{\Sigma}_2^T \mathbf{L}_k^{(2)})^{-1} (\mathbf{L}_k^{(1)T} \mathbf{L}_k^{(1)} + \mathbf{L}_k^{(2)T} \mathbf{L}_k^{(2)}), \\ \mathbf{L}_{k+1}^{(2)} &= \boldsymbol{\Sigma}_2 \boldsymbol{\Sigma}_2^T \mathbf{L}_k^{(2)} (\mathbf{L}_k^{(1)T} \boldsymbol{\Sigma}_1^2 \mathbf{L}_k^{(1)} + \mathbf{L}_k^{(2)T} \boldsymbol{\Sigma}_2 \boldsymbol{\Sigma}_2^T \mathbf{L}_k^{(2)})^{-1} (\mathbf{L}_k^{(1)T} \mathbf{L}_k^{(1)} + \mathbf{L}_k^{(2)T} \mathbf{L}_k^{(2)}), \end{aligned} \quad (\text{B.1})$$

which means

$$\begin{aligned} \mathbf{L}_{k+1}^{(1)} &= \frac{\boldsymbol{\Sigma}_1^2}{(\sigma_r - \varepsilon)^2} \mathbf{L}_k^{(1)} (\mathbf{L}_k^{(1)T} \frac{\boldsymbol{\Sigma}_1^2}{(\sigma_r - \varepsilon)^2} \mathbf{L}_k^{(1)} + \mathbf{L}_k^{(2)T} \frac{\boldsymbol{\Sigma}_2 \boldsymbol{\Sigma}_2^T}{(\sigma_r - \varepsilon)^2} \mathbf{L}_k^{(2)})^{-1} (\mathbf{L}_k^{(1)T} \mathbf{L}_k^{(1)} + \mathbf{L}_k^{(2)T} \mathbf{L}_k^{(2)}), \\ \mathbf{L}_{k+1}^{(2)} &= \frac{\boldsymbol{\Sigma}_2 \boldsymbol{\Sigma}_2^T}{(\sigma_r - \varepsilon)^2} \mathbf{L}_k^{(2)} (\mathbf{L}_k^{(1)T} \frac{\boldsymbol{\Sigma}_1^2}{(\sigma_r - \varepsilon)^2} \mathbf{L}_k^{(1)} + \mathbf{L}_k^{(2)T} \frac{\boldsymbol{\Sigma}_2 \boldsymbol{\Sigma}_2^T}{(\sigma_r - \varepsilon)^2} \mathbf{L}_k^{(2)})^{-1} (\mathbf{L}_k^{(1)T} \mathbf{L}_k^{(1)} + \mathbf{L}_k^{(2)T} \mathbf{L}_k^{(2)}). \end{aligned}$$

Clearly it holds that

$$\|\mathbf{L}_{k+1}^{(2)}\|_2 \leq \frac{\sigma_{r+1}^2}{(\sigma_r - \varepsilon)^2} \|\mathbf{L}_k^{(2)}\|_2 \quad (\text{B.2})$$

under the condition that

$$\mathbf{L}_k^{(1)T} \mathbf{L}_k^{(1)} + \mathbf{L}_k^{(2)T} \mathbf{L}_k^{(2)} \leq \mathbf{L}_k^{(1)T} \frac{\boldsymbol{\Sigma}_1^2}{(\sigma_r - \varepsilon)^2} \mathbf{L}_k^{(1)} + \mathbf{L}_k^{(2)T} \frac{\boldsymbol{\Sigma}_2 \boldsymbol{\Sigma}_2^T}{(\sigma_r - \varepsilon)^2} \mathbf{L}_k^{(2)}. \quad (\text{B.3})$$

If $\mathbf{L}_k^{(1)}$ is nonsingular, then (B.3) implies

$$(\mathbf{L}_k^{(2)} \mathbf{L}_k^{(1)-1})^T (\mathbf{I} - \frac{\boldsymbol{\Sigma}_2 \boldsymbol{\Sigma}_2^T}{(\sigma_r - \varepsilon)^2}) (\mathbf{L}_k^{(2)} \mathbf{L}_k^{(1)-1}) \leq \frac{\boldsymbol{\Sigma}_1^2}{(\sigma_r - \varepsilon)^2} - \mathbf{I}. \quad (\text{B.4})$$

It follows to see that

$$\|\mathbf{L}_k^{(2)} \mathbf{L}_k^{(1)-1}\|_2 \leq \sqrt{\frac{\sigma_r^2 - (\sigma_r - \varepsilon)^2}{(\sigma_r - \varepsilon)^2 - \sigma_{\min}^2}} \quad (\text{B.5})$$

is a sufficient condition of (B.4).

Next we will prove that if the initial guess \mathbf{L}_0 satisfies condition (B.5), then $\mathbf{L}_k^{(1)}$ is nonsingular and (B.2) is satisfied at every iteration k .

Provided that \mathbf{L}_0 satisfies (B.5), we obtain

$$\|\mathbf{L}_1^{(2)}\|_2 \leq \frac{\sigma_{r+1}^2}{(\sigma_r - \varepsilon)^2} \|\mathbf{L}_0^{(2)}\|_2. \quad (\text{B.6})$$

And according to the proof of Theorem 1, we know $\mathbf{L}_1^{(1)}$ is also nonsingular, which implies

$$\mathbf{L}_1^{(1)T} \boldsymbol{\Sigma}_1^2 \mathbf{L}_1^{(1)} + \mathbf{L}_1^{(2)T} \boldsymbol{\Sigma}_2 \boldsymbol{\Sigma}_2^T \mathbf{L}_1^{(2)}$$

is positive definite. Then by (B.1), we have

$$\|\mathbf{L}_1^{(2)} \mathbf{L}_1^{(1)-1}\|_2 \leq \|\boldsymbol{\Sigma}_2 \boldsymbol{\Sigma}_2^T \mathbf{L}_0^{(2)} \mathbf{L}_0^{(1)-1} \boldsymbol{\Sigma}_1^{-2}\|_2 \leq \frac{\sigma_{r+1}^2}{\sigma_r^2} \|\mathbf{L}_0^{(2)} \mathbf{L}_0^{(1)-1}\|_2 \leq \sqrt{\frac{\sigma_r^2 - (\sigma_r - \varepsilon)^2}{(\sigma_r - \varepsilon)^2 - \sigma_{\min}^2}}. \quad (\text{B.7})$$

Analogously, we can prove that for every iteration k , $\mathbf{L}_k^{(1)}$ is nonsingular, i.e., $\mathbf{L}_k^{(1)T} \boldsymbol{\Sigma}_1^2 \mathbf{L}_k^{(1)} + \mathbf{L}_k^{(2)T} \boldsymbol{\Sigma}_2 \boldsymbol{\Sigma}_2^T \mathbf{L}_k^{(2)}$ is positive definite, and (B.5) is satisfied. Since (B.5) is a sufficient condition of (B.4) and (B.3), inequality (B.2) is true at every iteration k , which implies that

$$\lim_{k \rightarrow 0} \|\mathbf{L}_k \mathbf{L}_k^\dagger - \mathbf{U}_1 \mathbf{U}_1^T\|_2 = 0.$$

The rest part of the proof is analogous to the proof of Theorem 1, which is omitted for brevity. \square

C Proof of Theorem 3

In Algorithm 4, $\mathbf{U}^{(n)}$ is obtained from the rank- R_n approximation of $\mathbf{A}_{(n)}$, which is done in an iterative manner and allows a tolerance parameter η_n . Therefore, we have

$$\|\mathbf{A}_{(n)} - \mathbf{L}^* \mathbf{R}^{*T}\|_F^2 \leq \eta_n^2 \|\mathbf{A}\|_F^2 + \gamma_n, \quad (\text{C.1})$$

where \mathbf{L}^* and \mathbf{R}^* are the same as in Algorithm 4. Note that \mathbf{R} is updated by solving a multi-side least squares problem

$$\min_{\mathbf{R}} \|\mathbf{A}_{(n)} - \mathbf{L} \mathbf{R}^T\|_F,$$

whose exact solution is $\mathbf{R} = \mathbf{A}_{(n)}^T (\mathbf{L}^\dagger)^T$. Thus

$$\|\mathbf{A}_{(n)} - \mathbf{L}^* \mathbf{R}^{*T}\|_F = \|\mathbf{A}_{(n)} - \mathbf{L}^* \mathbf{L}^{*\dagger} \mathbf{A}_{(n)}\|_F, \quad (\text{C.2})$$

where $\mathbf{L}^* \mathbf{L}^{*\dagger}$ represents an orthogonal projection on subspace $\mathcal{R}(\mathbf{L}^*)$. Consequently, by (C.1), (C.2) and (4.3), we have

$$\|\hat{\mathbf{A}} - \mathbf{A}\|_F^2 \leq \sum_{n=1}^N (\eta_n^2 \|\mathbf{A}_{(n)}\|_F^2 + \gamma_n),$$

which means

$$\frac{\|\hat{\mathbf{A}} - \mathbf{A}\|_F^2}{\|\mathbf{A}\|_F^2} \leq \sum_{n=1}^N (\eta_n^2 + \frac{\gamma_n}{\|\mathbf{A}\|_F^2}).$$

Combining with (4.3), we obtain (4.4).

The error analysis of Algorithm 5 can be analogously done. \square